

Refractive effects and Airy structure in inelastic $^{16}\text{O}+^{12}\text{C}$ rainbow scattering

S. Ohkubo^{1,2}, Y. Hirabayashi³, A. A. Ogloblin⁴, Yu. A. Gloukhov⁴,
A. S. Dem'yanova⁴ and W. H. Trzaska⁵

¹*Research Center for Nuclear Physics, Osaka University, Ibaraki, Osaka 567-0047, Japan*

²*University of Kochi, Kochi 780-8515, Japan*

³*Information Initiative Center, Hokkaido University, Sapporo 060-0811, Japan*

⁴*RSC "Kurchatov Institute", RU-123182 Moscow, Russia and*

⁵*JYFL, FIN-40351 Jyväskylä, Finland*

(Dated: December 24, 2014)

Inelastic $^{16}\text{O} + ^{12}\text{C}$ rainbow scattering to the 2^+ (4.44 MeV) state of ^{12}C was measured at the incident energies, $E_L = 170, 181, 200, 260$ and 281 MeV. A systematic analysis of the experimental angular distributions was performed using the coupled channels method with an extended double folding potential derived from realistic wave functions for ^{12}C and ^{16}O calculated with a microscopic α cluster model and a finite-range density-dependent nucleon-nucleon force. The coupled channels analysis of the measured inelastic scattering data shows consistently some Airy-like structure in the inelastic scattering cross sections for the first 2^+ state of ^{12}C , which is somewhat obscured and still not clearly visible in the measured data. The Airy minimum was identified from the analysis and the systematic energy evolution of the Airy structure was studied. The Airy minimum in inelastic scattering is found to be shifted backward compared with that in elastic scattering.

PACS numbers: 25.70.Bc, 24.10.Eq, 24.10.Ht,

I. INTRODUCTION

Since the first observation of a nuclear rainbow in elastic α particle scattering from ^{58}Ni [1], the importance of the concept of rainbow scattering in studies of nuclear reactions and structures has been widely understood [2–4]. The interaction potential can be determined without discrete ambiguity up to the internal region by studying rainbow scattering because refraction carries information from the inner region. The nuclear rainbow has been observed under weak absorption in many systems and has been extensively studied [2]. The uniquely determined interaction potential made it possible to study the cluster structure of the compound system above and below the threshold energy by unifying unbound and bound states as typically shown for the $\alpha+^{16}\text{O}$ and $\alpha+^{40}\text{Ca}$ systems [4]. The nuclear rainbow has also been observed for typical heavy ion systems such as $^{16}\text{O}+^{16}\text{O}$, $^{16}\text{O}+^{12}\text{C}$ and $^{12}\text{C}+^{12}\text{C}$, for which the higher order Airy structure has been clearly observed [3, 5–10]. The interaction potential uniquely determined for the most typical $^{16}\text{O}+^{16}\text{O}$ system made it possible to understand the superdeformed $^{16}\text{O}+^{16}\text{O}$ cluster structure in ^{32}S and the nuclear rainbow in a unified way [11, 12].

The nuclear rainbow has also been observed for inelastic scattering [2, 13–17]. The rainbow in inelastic rainbow scattering makes it possible to understand the interaction potential for the inelastic channels up to the internal region. For typical $\alpha+^{40}\text{Ca}$ and $^6\text{Li}+^{12}\text{C}$ systems [18, 19], the mechanism of the nuclear rainbow and the Airy structure in inelastic scattering has been studied [19, 20]. Inelastic rainbow scattering has also been especially powerful in understanding the highly excited cluster structure near and above the threshold energy, such as the α particle condensation of the Hoyle state in

^{12}C and the Hoyle-analog state in ^{16}O [21–25]. A recent systematic study of the evolution of the Airy structure in inelastic scattering for the typical $\alpha+^{16}\text{O}$ system [26] showed that the cluster structure with core excitation in ^{20}Ne near the threshold energy region and the inelastic nuclear rainbow scattering can be understood in a unified way by using reliable interaction potentials for the inelastic channels. This urges us to study inelastic rainbow scattering with heavy ions in order to determine the interaction potentials in inelastic channels, which will make it possible to understand the molecular structure with core excitation, for which phenomenological shallow potentials have been used widely instead of a deep potential [27].

For heavy ion systems, an inelastic nuclear rainbow has been observed for $^{16}\text{O}+^{16}\text{O}$, $^{16}\text{O}+^{12}\text{C}$ and $^{12}\text{C}+^{12}\text{C}$ scattering [2, 13–17]. For the typical $^{16}\text{O}+^{16}\text{O}$ system, Khoa *et al.* [16] could trace a weak rainbow pattern in the energy range from 350–704 MeV, however, a clear identification of the Airy minimum and its energy evolution was not possible. For the asymmetric $^{16}\text{O}+^{12}\text{C}$ system, elastic scattering angular distributions have been measured without being obscured due to symmetrization over a wide range of incident energies at $E_L = 62$ –1503 MeV [6–10, 17, 28]. Very recently, evidence for a secondary bow in elastic scattering caused by coupling to the inelastic channel has been reported [29]. Therefore it is particularly intriguing to study inelastic rainbow scattering for this system.

The purpose of this paper is to study the existence and evolution of the Airy structure in inelastic rainbow scattering by analyzing the measured inelastic and elastic angular distributions of differential cross sections with an extended double folding model by using realistic wave functions for ^{12}C and ^{16}O obtained in the microscopic

cluster model calculations.

II. EXPERIMENT

Differential cross-sections of inelastic $^{16}\text{O}+^{12}\text{C}$ scattering at $E_L = 170\text{--}280$ MeV leading to the 2^+ (4.44 MeV) state of ^{12}C were measured at the cyclotron of Jyväskylä University (Finland). ^{16}O beams with an intensity of about 100 nA (electrical) were exploited. The energetic resolution of the beam was $\approx 0.3\%$, and the size of the beam spot on the target was about $2\text{ mm} \times 3\text{ mm}$. The targets were self-supporting carbon foils of 0.3 mg/cm^2 thickness. A scattering chamber of diameter $\approx 1500\text{ mm}$ was used in the experiment. Detectors were located on rotating tables, so the full angular range could be covered. Differential cross-sections at forward angles ($\theta_{c.m.} = 7\text{--}40^\circ$) were measured by a $\Delta E - E$ telescope of semiconductor counters. The thickness of E and ΔE counters was $600\text{--}800$ and $20\text{--}40\text{ }\mu\text{m}$, respectively. The solid angle covered by the telescope was about 0.08 milliradian. The total energy resolution (determined mainly by kinematics) was 1.2 MeV . The angular resolution was $\pm 0.2^\circ$ and determined mainly by the beam angular spread. For measurements at larger angles with $\theta_{c.m.} > 40^\circ$, a position-sensitive $\Delta E - E$ detector was used. It included a gas-filled proportional ΔE counter with variable pressure, and an E detector which consists of ten silicon pin-diodes of $10\text{ mm} \times 10\text{ mm}$ dimension each with thickness of $370\text{--}760\text{ }\mu\text{m}$. This detector could cover an angular range of about 10° in the laboratory system. The accuracy of the absolute cross-section measurements was estimated to be around 15% .

III. COUPLED CHANNELS ANALYSIS

We study $^{16}\text{O}+^{12}\text{C}$ scattering with the coupled channels method using an extended double folding (EDF) model that describes all the diagonal and off-diagonal coupling potentials derived from the microscopic realistic wave functions for ^{12}C and ^{16}O using a density-dependent nucleon-nucleon force. The diagonal and coupling potentials for the $^{16}\text{O}+^{12}\text{C}$ system are calculated using the EDF model without introducing a normalization factor:

$$V_{ij,kl}(\mathbf{R}) = \int \rho_{ij}^{(^{16}\text{O})}(\mathbf{r}_1) \rho_{kl}^{(^{12}\text{C})}(\mathbf{r}_2) \times v_{NN}(E, \rho, \mathbf{r}_1 + \mathbf{R} - \mathbf{r}_2) d\mathbf{r}_1 d\mathbf{r}_2, \quad (1)$$

where $\rho_{ij}^{(^{16}\text{O})}(\mathbf{r})$ is the diagonal ($i = j$) or transition ($i \neq j$) nucleon density of ^{16}O taken from the microscopic $\alpha+^{12}\text{C}$ cluster model wave functions calculated with the orthogonality condition model (OCM) in Ref. [30]. This model uses a realistic size parameter both for the α particle and ^{12}C and is an extended version of the OCM α cluster model of Ref. [31], which reproduces

almost all the energy levels well up to $E_x \approx 13\text{ MeV}$ and the electric transition probabilities in ^{16}O . The calculated $B(E2 : 2_1^+ \rightarrow 0_1^+)$, $7.5\text{ e}^2\text{fm}^4$, agrees well with the experimental data, $7.6\text{ e}^2\text{fm}^4$ [30]. We take into account the important transition densities available in Ref. [30], i.e., $g.s \leftrightarrow 3^-$ (6.13 MeV) and 2^+ (6.92 MeV) in addition to all the diagonal densities. $\rho_{kl}^{(^{12}\text{C})}(\mathbf{r})$ represents the diagonal ($k = l$) or transition ($k \neq l$) nucleon density of ^{12}C calculated using the microscopic three α cluster model in the resonating group method [32]. This model reproduces the structure of ^{12}C well and the wave functions have been checked for many experimental data, including charge form factors and electric transition probabilities [32]. The calculated $B(E2 : 2_1^+ \rightarrow 0_1^+)$, $9.3\text{ e}^2\text{fm}^4$ and $B(E3 : 3^- \rightarrow 0_1^+)$, $124\text{ e}^2\text{fm}^6$, agree well with the experimental data, $7.8\text{ e}^2\text{fm}^4$ and $107\text{ e}^2\text{fm}^6$, respectively [32]. In the coupled channels calculations we take into account the 0_1^+ (0.0 MeV), 2^+ (4.44 MeV), and 3^- (9.64 MeV) states of ^{12}C . The mutual excitation channels in which both ^{12}C and ^{16}O are excited simultaneously are not included. For the effective interaction v_{NN} we use the DDM3Y-FR interaction [33], which takes into account the finite-range exchange effect [34]. An imaginary potential (non-deformed) is introduced phenomenologically for all the diagonal potentials to take into account the effect of absorption due to other channels, which was successful in the recent coupled channels studies of $^{16}\text{O}+^{12}\text{C}$ rainbow scattering [29, 35]. Off-diagonals are assumed to be real.

In Fig. 1 angular distributions of elastic and inelastic $^{16}\text{O}+^{12}\text{C}$ scattering at $E_L = 170\text{--}281\text{ MeV}$, calculated using the coupled channels method including coupling to the 2^+ and 3^- states of ^{12}C and ^{16}O , are displayed in comparison with the measured experimental data. The same imaginary potentials are used for all the channels for simplicity. The potential parameters used and the values of the volume integral per nucleon pair of the double folding (DF) potential, J_V , are given in Table I. We found that the DF potential works well without introducing a normalization factor. The values of the volume integral per nucleon pair are consistent with those used in other DF optical model calculations [7, 8, 34, 36]. The DF potentials used belong to the same global potential family found in the $E_L = 62\text{--}124\text{ MeV}$ [7] and $E_L = 132\text{--}1503\text{ MeV}$ regions [8, 34]. The agreement with the experimental data in elastic scattering is comparable to the optical model calculations in Refs. [8, 10]. The evolution of the Airy minimum in elastic scattering is consistent with that in the lower energy region $62\text{--}124\text{ MeV}$ [7] and $132\text{--}260\text{ MeV}$ [8] studied with the single channel optical potential model. The calculated elastic scattering cross sections are decomposed into farside and nearside components. We see that the angular distributions are dominated by the refractive farside scattering in this energy region. This means that inelastic scattering in the energy region is dominated by refractive waves. In fact, we have confirmed that inelastic scattering to the 0_2^+ state at 7.65 MeV , for which the decomposition of the calculated

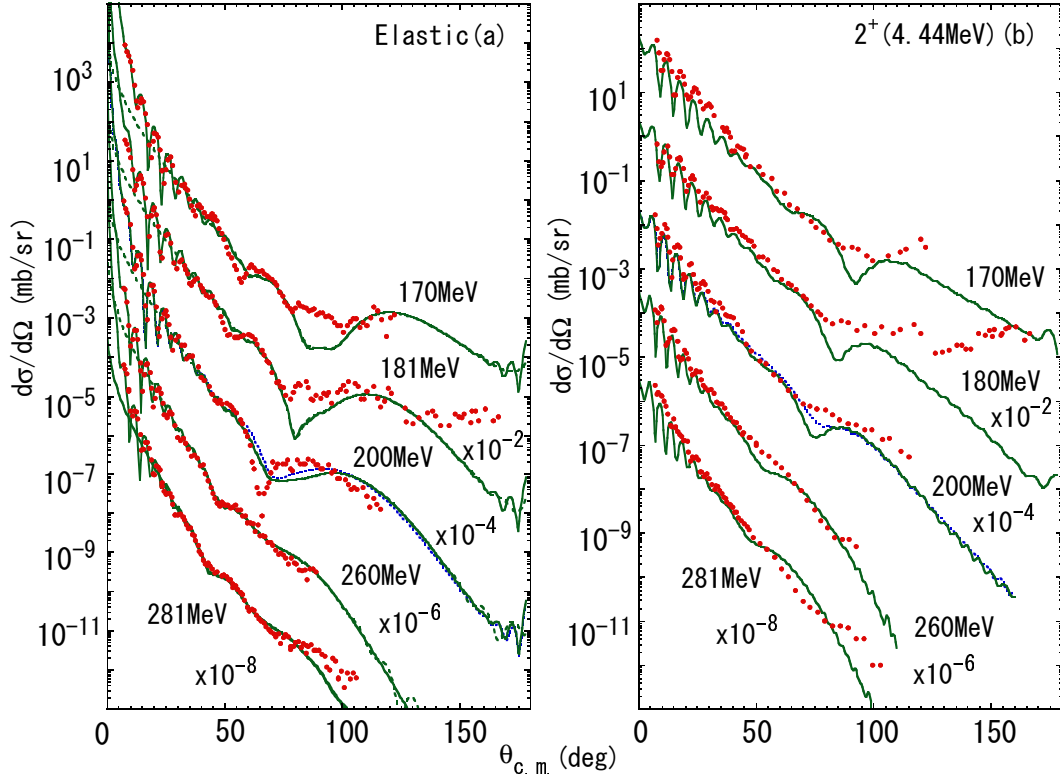


FIG. 1: (Color online) Angular distributions in $^{16}\text{O}+^{12}\text{C}$ (a) elastic and (b) inelastic scattering to the 2^+ state of ^{12}C calculated using the coupled channels method including coupling to the 2^+ and 3^- states of ^{12}C and ^{16}O with the imaginary potentials in Table I (solid lines) are compared with the experimental data (points). The green dashed lines in elastic scattering display the calculated farside components. The blue dotted lines at 200 MeV are calculated with a channel dependent imaginary potential for the 2^+ and 3^- states of ^{12}C (see text). The elastic scattering data are from Refs. [8, 10].

scattering amplitude into its farside and nearside components is much easier because of no magnetic substates, is also dominated by farside refractive scattering. The characteristic features of the experimental angular distributions in inelastic scattering are reproduced well by the calculations. We see a clear minimum caused by refractive inelastic scattering in the $\theta_{c.m.}=95\text{--}85^\circ$ region of the calculated angular distributions at 170 and 181 MeV, which makes it possible to identify the Airy minimum at $\theta_{c.m.}\approx 87$ and 83° , respectively, in the experimental angular distributions in inelastic rainbow scattering. At 200 and 260 MeV the Airy minimum is also seen at $\theta_{c.m.}\approx 75$ and 53° in the calculated angular distributions, respectively, although the corresponding minimum is fading in the experimental angular distributions.

In order to see the persistence and evolution of the Airy minimum clearly at the higher energies, which is obscured by the imaginary potential, we show in Fig. 2 the elastic and inelastic scattering angular distributions at 281 MeV calculated with the real potential in Table I but switching off the imaginary potential. Very recently it has been reported [29] that the Airy minimum in Fig. 2(a) at $\theta_{c.m.}\approx 65^\circ$ is caused by the coupling to the 2^+ state of ^{12}C and that coupling to the other excited states of ^{12}C and ^{16}O plays a role to obscure this Airy

TABLE I:

The volume integral per nucleon pair J_V of the DF potential and the imaginary potential parameters used in the coupled channels calculations in Fig. 1.

E_L (MeV)	J_V (el) (MeV fm ³)	W_V (MeV)	R_V (fm)	a_V (fm)	J_V (inel) (MeV fm ³)
170	306	15.5	5.7	0.65	303
181	304	16.5	5.7	0.55	301
200	301	18.0	5.6	0.65	298
260	290	18.5	5.6	0.60	287
281	285	18.0	5.6	0.60	283

minimum improving the agreement with the experimental data in the relevant angular region. The role of the 2^+ state of ^{12}C is clearly seen in Fig. 2(a) in the calculations where the imaginary potential is switched off. The Airy minimum caused by the coupling to the 2^+ state of ^{12}C (dashed line) is much clearer. The Airy minimum at $\theta_{c.m.}\approx 40^\circ$ in Fig. 2(a) appears even in the single channel calculation (dotted line). The full coupled channels calculation with coupling to the 2^+ and 3^- states of ^{12}C and ^{16}O without the imaginary potential (solid line)

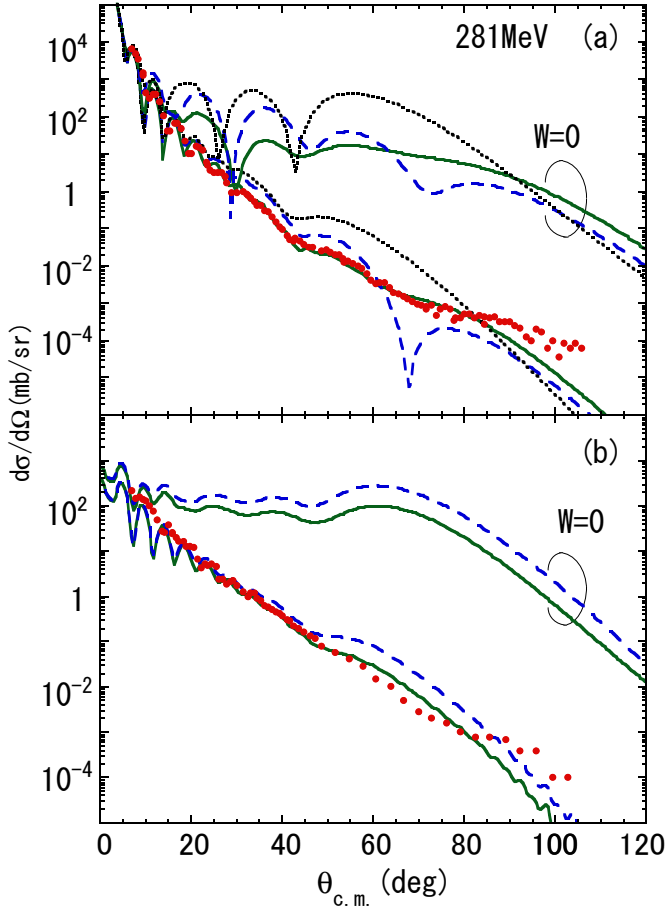


FIG. 2: (Color online) Angular distributions in $^{16}\text{O}+^{12}\text{C}$ (a) elastic and (b) inelastic scattering to the 2^+ state of ^{12}C at $E_L=281$ MeV calculated using the coupled channels method with the imaginary potentials in Table I are compared with those calculated by switching off the imaginary potential and the experimental data (points). The solid and dashed lines represent the coupled channels calculations with coupling to the 2^+ and 3^- states of ^{12}C and ^{16}O , and those with coupling to the 2^+ state of ^{12}C only, respectively. The dotted lines represent the single channel calculation.

gives an Airy minimum at $\theta_{c.m.} \approx 40^\circ$, which is similar to the single channel calculation. Thus the Airy minimum at $\theta_{c.m.} \approx 40^\circ$ is an ordinary nuclear rainbow caused by the refractive DF potential, and the Airy minimum at the larger angle $\theta_{c.m.} \approx 65^\circ$ in Fig. 2(a) was claimed to be a new kind of Airy minimum of a secondary rainbow dynamically caused predominantly by coupling to the deformed 2^+ state of ^{12}C [29]. The role of the excitation to the 2^+ state of ^{12}C was also investigated at other energies using the potential parameters in Table I. On the other hand, as for the inelastic scattering to the 2^+ state of ^{12}C , the calculations without the imaginary potential in Fig. 2(b) show an Airy minimum at $\theta_{c.m.} \approx 47^\circ$. Thus the small minimum at $\theta_{c.m.} \approx 47^\circ$ in the experimental angular distribution, which is close to the Airy minimum in elastic scattering, is assigned to be an Airy minimum

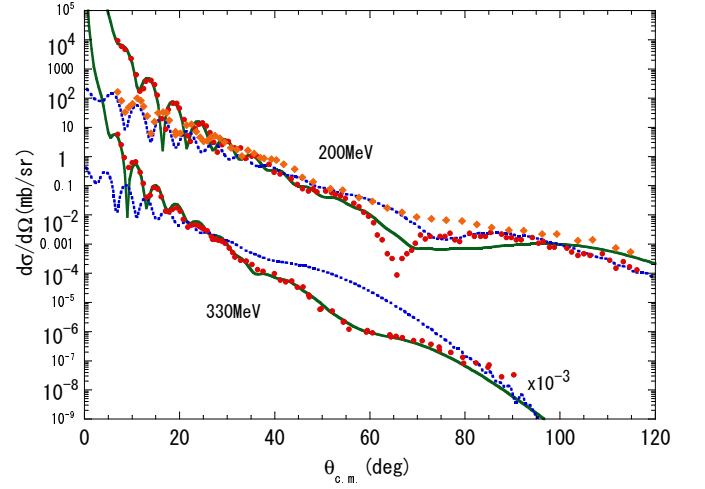


FIG. 3: (Color online) Angular distributions in inelastic $^{16}\text{O}+^{12}\text{C}$ scattering to the 2^+ state of ^{12}C (dotted line) and elastic scattering (solid line) at 200 MeV and 330 MeV calculated using the coupled channels method including coupling to the 2^+ and 3^- states of ^{12}C and ^{16}O are compared with the experimental inelastic (squares) and elastic (points) data [37]. For 330 MeV the potential parameters in Table I of Ref. [29] are used.

in inelastic scattering. The Airy minimum in inelastic scattering at 260, 200, 180 and 170 MeV can be similarly located at $\theta_{c.m.} \approx 53, 75, 83$ and 87° , respectively. The broad Airy maximum at 281 MeV seen clearly in Fig. 2(b) in the calculations without the imaginary potentials, centered at $\theta_{c.m.} \approx 60^\circ$, seems to have some effect on the elastic scattering.

To show that the inelastic scattering to the 2^+ state of ^{12}C is more enhanced than the elastic scattering, the experimental and calculated angular distributions at 200 and 330 MeV are compared in Fig. 3. At 200 MeV we see that the observed cross sections in inelastic scattering are larger than those in elastic scattering in the intermediate angular region. Also, at 330 MeV the calculated inelastic scattering is greatly enhanced compared with the observed elastic scattering cross sections at intermediate angles. We note that the broad peak of the Airy maximum in inelastic scattering appears in the angular region where the Airy minimum appears at $\theta_{c.m.} \approx 60^\circ$ in elastic scattering. The coupling between the elastic scattering and inelastic scattering has a large effect on the behavior of the angular distributions in the relevant angular region and causes a new kind of dynamically induced Airy minimum in elastic scattering [29].

In Fig. 4 the energy evolution of the angles of the Airy minimum in elastic scattering and inelastic scattering is displayed as a function of inverse c.m. energies. We see that the Airy minimum in inelastic scattering is slightly shifted toward the larger angles. This shift is caused by the excitation energy effect as discussed in Ref. [19], because the size of the 2^+ state of ^{12}C is almost as large as that of the band head ground state 0^+ . This is confirmed

by the volume integrals in Table I, which are almost the same for elastic and inelastic scattering. The positions of the Airy minima in inelastic scattering are approximately on the straight line similar to those in elastic scattering [10], which gives a support to the present assignment of the Airy minimum in inelastic scattering.

In Fig. 5 we show the calculated angular distributions in elastic and inelastic $^{16}\text{O}+^{12}\text{C}$ scattering at $E_L=350$ -608 MeV. The imaginary potentials were interpolated from Table I in Ref. [29]. The calculations predict an Airy minimum of the secondary bow in elastic scattering caused by coupling to the inelastic channels at the higher energies such as a clear Airy minimum at 400 MeV. On the other hand, in inelastic scattering the emergence of the Airy minimum seems obscured because of absorption. However, the rainbow pattern with the Airy maximum accompanying the fall-off of the cross sections toward the large angles, which was discussed for the $^{16}\text{O}+^{16}\text{O}$ system by Khoa *et al.* [16], persists. Because the dynamical Airy minimum in elastic scattering is mostly brought about by coupling to the 2^+ state of ^{12}C [29], the appearance of this Airy minimum, for example at 400 MeV, seems to be related to the persistence of the nuclear rainbow in inelastic scattering to the 2^+ state. At 608 MeV, the experimental angular distribution of Brandan *et al.* [17] shows the fall-off of the cross sections both in elastic and inelastic scattering and no Airy minimum is confirmed. At 608 MeV, a dynamical Airy minimum of the secondary bow in elastic scattering is no longer perceptible, even in the calculations with $W_V = 0$, suggesting that the cou-

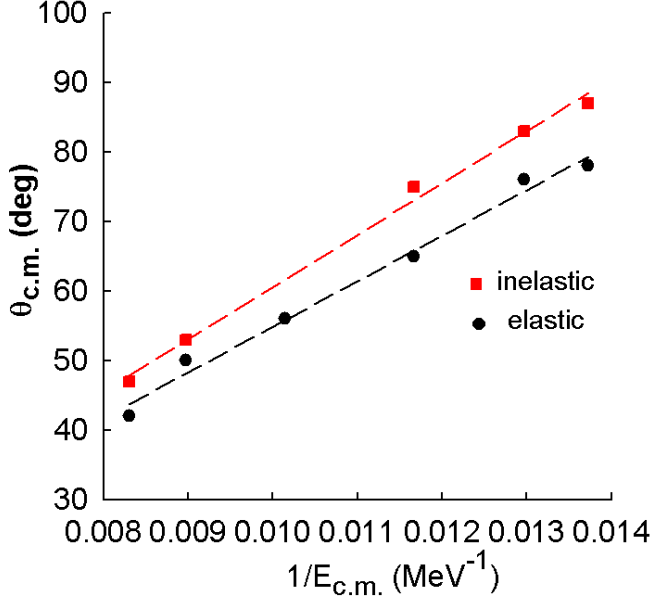


FIG. 4: (Color online) The positions of the Airy minimum observed in inelastic scattering to the 2^+ state of ^{12}C (filled square) and elastic scattering (filled circle) of $^{16}\text{O}+^{12}\text{C}$ are displayed as a function of the inverse c.m. energies. The lines are drawn by fitting the data.

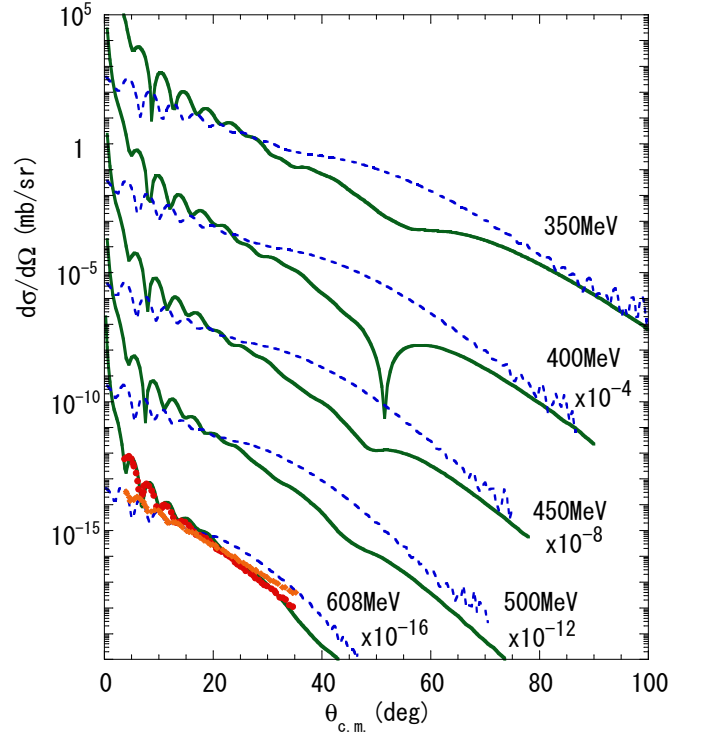


FIG. 5: (Color online) Angular distributions in $^{16}\text{O}+^{12}\text{C}$ elastic (solid line) and inelastic scattering to the 2^+ state of ^{12}C (dashed line) at $E_L=350, 400, 450, 500$ and 608 MeV calculated using the coupled channels method including coupling to the 2^+ and 3^- states of ^{12}C and ^{16}O . The experimental data (points) at 608 MeV are taken from Ref. [17].

pling to the 2^+ state is not of specific importance in this high energy region.

Finally we discuss the reasons of the obscurity of the experimental Airy minimum in the inelastic scattering data compared with calculated results. The contribution of the α particle transfer is not important for the obscurity of the Airy minimum. In fact, the coupled reaction channels calculations of $^{16}\text{O}+^{12}\text{C}$ scattering in Ref. [38] showed that it is more than three orders of magnitude smaller than the experimental data in the relevant angular region. We note that the present calculations take into account the one nucleon exchange effect, which is suggested to prevail over other transfer reactions [38], by using effective interaction DDM3Y, in which the knock-on exchange effect is incorporated [3, 33]. As for the coupling to the other excited states of ^{12}C such as the 0_2^+ , 0_3^+ , and 2_2^+ states, we have confirmed in the extended coupled channels calculations that its contribution to the Airy minimum in inelastic scattering is not significant. In the present calculations mutual excitations, in which both the 2^+ of ^{12}C and the excited states of ^{16}O are excited simultaneously, are not included. To take into account the flow of the flux via the 2^+ state of ^{12}C to the excited 2^+ and 3^- states of ^{16}O phenomenologically, in Fig. 1 angular distributions calculated by using a slightly stronger imaginary potential ($W_V = 24$, $R_V=5.0$ and $a_V=0.8$)

for the channels are displayed at 200 MeV by the blue dotted lines. We see that the calculated Airy minimum preceding the first Airy maximum (the broad rainbow shoulder) is obscured significantly in close to the experimental data by this imaginary potential effect. Because a phenomenological imaginary potential cannot correctly replace a microscopic treatment of coupling as was discussed for a secondary bow in Ref. [29] and ripples in the nuclear rainbow in Ref. [35], an accurate microscopic treatment of these channels coupling may be necessary to investigate the further obscurity of the Airy minimum of the experimental data.

IV. SUMMARY

Inelastic $^{16}\text{O} + ^{12}\text{C}$ rainbow scattering to the 2^+ (4.44 MeV) state of ^{12}C was measured at $E_L = 170\text{--}281$ MeV. A systematic analysis of the existence and evolution of the Airy minimum in the angular distributions in inelastic rainbow scattering was done using the coupled channels method with an extended double folding potential derived from the realistic wave functions for ^{12}C and ^{16}O calculated with a microscopic α cluster model with a finite-range density-dependent nucleon-nucleon force.

The coupled channels analysis of the measured inelastic $^{16}\text{O} + ^{12}\text{C}$ scattering data shows consistently some Airy-like structure in the inelastic scattering cross sections for the first 2^+ state of ^{12}C , which is somewhat obscured and still not clearly visible in the measured data. The Airy minimum was identified from the analysis and it was found that the Airy minimum in inelastic scattering is shifted backward compared with that in elastic scattering. The existence of rainbows in inelastic scattering seems to be responsible for creating a dynamical Airy minimum of the secondary rainbow in elastic scattering. It is intriguing to study the Airy minimum in inelastic heavy ion rainbow scattering experimentally and theoretically and to reveal the relationship between the dynamically induced secondary bow in elastic scattering and the structure of the involved nuclei.

The work was partly supported by Russian Scientific Foundation (Grant No. RNF14-12-00079). Two of the authors (S.O. and Y.H.) would like to thank the Yukawa Institute for Theoretical Physics for the hospitality extended during a stay in 2014. Part of this work was supported by the Grant-in-Aid for the Global COE Program “The Next Generation of Physics, Spun from Universality and Emergence” from the Ministry of Education, Culture, Sports, Science and Technology (MEXT) of Japan.

-
- [1] D. A. Goldberg, S. M. Smith, and G. F. Burdzyk, *Phys. Rev. C* **10**, 1362 (1974).
 - [2] D. T. Khoa, W. von Oertzen, H. G. Bohlen, and S. Ohkubo, *J. Phys. G* **34**, R111 (2007).
 - [3] M. E. Brandan and G. R. Satchler, *Phys. Rep.* **285**, 143 (1997) and references therein.
 - [4] F. Michel, S. Ohkubo, and G. Reidemeister, *Prog. Theor. Phys. Suppl.* **132**, 7 (1998) and references therein.
 - [5] M. P. Nicoli *et al.*, *Phys. Rev. C* **60**, 064608 (1999).
 - [6] A. A. Ogloblin, Dao T. Khoa, Y. Kondō, Yu. A. Glukhov, A. S. Dem’yanova, M. V. Rozhkov, G. R. Satchler, and S. A. Goncharov, *Phys. Rev. C* **57**, 1797 (1998).
 - [7] M. P. Nicoli *et al.*, *Phys. Rev. C* **61**, 034609 (2000).
 - [8] A. A. Ogloblin *et al.*, *Phys. Rev. C* **62**, 044601 (2000).
 - [9] S. Szilner, M. P. Nicoli, Z. Basrak, M. Freeman, F. Haas, R. A. Morsad, M. E. Brandan, and G. R. Satchler, *Phys. Rev. C* **64**, 064614 (2001).
 - [10] A. A. Ogloblin, S. A. Goncharov, Yu. A. Glukhov, A. S. Dem’yanova, M. V. Rozhkov, V. P. Rudakov, and W. H. Trzaska, *Phys. At. Nucl.* **66**, 1478 (2003).
 - [11] S. Ohkubo and K. Yamashita, *Phys. Rev. C* **66**, 021301(R) (2002).
 - [12] S. Ohkubo, *Proceedings of Symposium on Nuclear Clusters: From light exotic to superheavy nuclei*, edited by J. Jolos and W. Scheid, (EP Systema, Debrecen, Hungary 2003) p.161; S. Ohkubo, *Heavy Ion Physics* **18**, 287 (2003).
 - [13] H. G. Bohlen, M. R. Clover, G. Ingold, H. Lettau, and W. von Oertzen, *Z. Phys. A* **308**, 121 (1982).
 - [14] H. G. Bohlen, X. S. Chen, J. G. Cramer, P. Fröbrich, B. Gebauer, H. Lettau, A. Miczaika, W. von Oertzen, R. Ulrich, and T. Wilpert, *Phys. A* **322**, 241 (1985).
 - [15] H. G. Bohlen, E. Stiliaris, B. Gebauer, W. von Oertzen, M. Wilpert, Th. Wilpert, A. Ostrowski, Dao T. Khoa, A.S. Demyanova, and A.A. Ogloblin, *Z. Phys. A* **346**, 189 (1993).
 - [16] D. T. Khoa, H. G. Bohlen, W. von Oertzen, G. Bartsch, A. Blazevic, F. Nuoffer, B. Gebauer, W. Mittig, and P. Roussel-Chomaz, *Nucl. Phys. A* **759**, 3 (2005).
 - [17] M. E. Brandan, A. Menchaca-Rocha, M. Buenerd, J. Chauvin, P. DeSaintignon, G. Duhamel, D. Lebrun, P. Martin, G. Perrin, and J. Y. Hostachy, *Phys. Rev. C* **34**, 1484 (1986).
 - [18] F. Michel and S. Ohkubo, *Eur. Phys. J. Special Topics* **150**, 41 (2007).
 - [19] F. Michel and S. Ohkubo, *Phys. Rev. C* **70**, 044609 (2004); *Nucl. Phys. A* **738**, 231 (2004).
 - [20] F. Michel and S. Ohkubo, *Phys. Rev. C* **72**, 054601 (2005).
 - [21] S. Ohkubo and Y. Hirabayashi, *Phys. Rev. C* **70**, 041602(R) (2004).
 - [22] S. Ohkubo and Y. Hirabayashi, *Phys. Rev. C* **75**, 044609 (2007).
 - [23] S. Ohkubo and Y. Hirabayashi, *Phys. Lett. B* **684**, 127 (2010).
 - [24] T. L. Belyaeva, A. N. Danilov, A. S. Dem’yanova, S. A. Goncharov, A. A. Ogloblin, and R. Perez-Torres, *Phys. Rev. C* **82**, 054618 (2010).
 - [25] Sh. Hamada, Y. Hirabayashi, N. Burtbayev, and S. Ohkubo, *Phys. Rev. C* **87**, 024311 (2013).
 - [26] Y. Hirabayashi and S. Ohkubo, *Phys. Rev. C* **88**, 014314 (2013).
 - [27] Y. Abe, Y. Kondō, and T. Matsuse, *Prog. Theor. Phys. Suppl.* **68**, 303 (1980) and references therein.

- [28] W. H. Trzaska, Phys. At. Nucl. **65**, 725 (2002).
- [29] S. Ohkubo and Y. Hirabayashi, Phys. Rev. C **89**, 051601(R) (2014).
- [30] S. Okabe, in *Tours Symposium on Nuclear Physics II*, edited by H. Utsunomiya *et al.* (World Scientific, Singapore, 1995), p. 112.
- [31] Y. Suzuki, Prog. Theor. Phys. **55**, 1751 (1976); Prog. Theor. Phys. **56**, 111 (1976).
- [32] M. Kamimura, Nucl. Phys. **A351**, 456 (1981).
- [33] A. M. Kobos, B. A. Brown, P. E. Hodgson, G. R. Satchler, and A. Budzanowski, Nucl. Phys. **A384**, 65 (1982); A. M. Kobos, B. A. Brown, R. Lindsay, and G. R. Satchler, Nucl. Phys. **A425**, 205 (1984). G. Bertsch, J. Borysowicz, H. McManus, and W. G. Love, Nucl. Phys. **A284**, 399(1977);
- [34] D. T. Khoa, W. von Oertzen, and H. G. Bohlen, Phys. Rev. C **49**, 1652 (1994).
- [35] S. Ohkubo and Y. Hirabayashi, Phys. Rev. C **89**, 061601(R) (2014).
- [36] M. E. Brandan *et al.*, Nucl. Phys. **A688**, 659 (2001).
- [37] A. S. Dem'yanova *et al.*, IAEA Database exfor, <http://www.nds.iaea.org/exfor/>.
- [38] A. T. Rudchik *et al.*, Eur. Phys. J. A **44**, 221 (2010).